Electron Density and Bonding in Ring Silicates: Beryl, Cordierite, Dioptase *

Elena L. Belokoneva and Vladimir G. Tsirel'son

Moscow State University and Mendeleev Institute of Chemical Technology, Moscow, Russia

Z. Naturforsch. **48a**, 41–46 (1993); received January 10, 1992

The electron density and bonding in the silicates beryl, cordierite and dioptase has been investigated. The replacement of Be, Si and Al atoms in the identical structural fragments leads to a $\delta\varrho$-redistribution and changes the σ-bond character from slightly polar to strongly polar. The condensation of $[SiO_4]$-tetrahedra in the rings leads to the accumulation of electron density near bridge oxygens. This phenomenon is expressed especially in dioptase (pure ring silicate). Therefore, the electron density picture may be considered as a supplementary independent criterion for classification of crystal structures. The experimental $\delta\varrho$-maps for H_2O molecules in dioptase are in good agreement with theoretical ones. The $\delta\varrho$-distribution of 3d-electrons and bonding in the Jahn-Teller distorted Cu-octahedron can be interpreted from crystal-field-theory point of view.

Key words: Electron density; Bonding; Ring silicates.

The investigation of the experimental electron density distribution obtained by precise X-ray data [1] offers the possibility to analyse the chemical bonding and its peculiarities in crystals, the atomic charges, the principles of classification of crystal structures and other crystal chemical concepts on a more fundamental level. The comparison of the experimental $\delta\varrho$-maps with theoretical ones is also very useful. A review of recent data on $\delta\varrho$-distributions in silicates [2] shows the relevance of this approach and the insufficiency of data concerning certain groups, in particular ring silicates.

New data on orthorhombic iron-rich low-cordierite $Na_{0.04}(Al_2Si)(Mg_{1.13}Fe_{0.78}Mn_{0.05}) \cdot [Al_2Si_4O_{18}] \cdot 0.2\,H_2O \cdot 0.06\,CO_2$ and trigonal dioptase $Cu_6Si_6O_{18} \cdot 6\,H_2O$ are presented in this work. Together with hexagonal beryl $Na_{0.04}Be_{2.98}Al_2[Si_6O_{18}] \cdot 0.3\,H_2O$ [2, 3] these three minerals are classified as ring silicates [4] possessing different symmetry of the tetrahedral anionic group $[T_6O_{18}]$. The cations Al, (Mg, Fe, Mn) and Cu have octahedral coordination. The minor impurity of water molecules in beryl and cordierite is established within the channels. At the same time, water molecules are considered as important structural elements in dioptase, forming rings of $6\,H_2O$ like $[Si_6O_{18}]$ (Figures 1a–c).

The experimental and data-treatment conditions are given in Table 1. The models used for refinement were based on the precise determination of the cordierite structure by Armbruster [5] and by Armbruster and Bürgi [6], and of the dioptase structure by Belov et al. [7]. The results of high-order refinement were the

Table 1. Crystallographic and experimental data.

	Beryl	Cordierite	Dioptase
a, Å	9.222 (3)	17.155 (5)	14.597 (2)
b, Å	9.222 (3)	9.777 (4)	14.597 (2)
c, Å	9.204 (1)	9.339 (1)	7.796 (14)
Sp. group	P6/mcc	C ccm	$R\bar{3}$
r_{sph}, cm	0.012	0.0125	0.01
No. refl., meas. ($I \geq 1.96\,\sigma_I$)	4971	6324	3878
Max. no. equiv.	12	4	3
Aver. stat., R_{int}	2.3	2.5	3.5
No. indep. refl.	752	1982	1593
Abs. corr., μ_r	0.1	0.33	0.7
Ext. corr., R_x (Zachariasen)	1566	6138	8414
Angle range for high-order refl., $\sin\theta/\lambda$	0.8–1.08	0.65–1.08	0.75–1.08
No. reflection	338	1058	625
R_{hkl}	0.73	1.18	1.90
R_{whkl}	0.79	1.19	2.00
S	1.020	1.023	0.862

Diffractometer P$\bar{1}$ "Syntex" λMo-Kα, graphite monochromator, 2θ–θ-step scan, 2–24 degree/min, $\sin\theta/\lambda_{max} = 1.08$ Å^{-1}, MINEXTL-complex of crystallographical programs [9]; independent-atom crystal model.

* Presented at the Sagamore X Conference on Charge, Spin, and Momentum Densities, Konstanz, Fed. Rep. of Germany, September 1–7, 1991.

Reprint requests to Dr. E. L. Belokoneva, Geological Faculty, Moscow State University, Moskva-119899, Russia.

0932-0784 / 93 / 0100-0041 $ 01.30/0. – Please order a reprint rather than making your own copy.

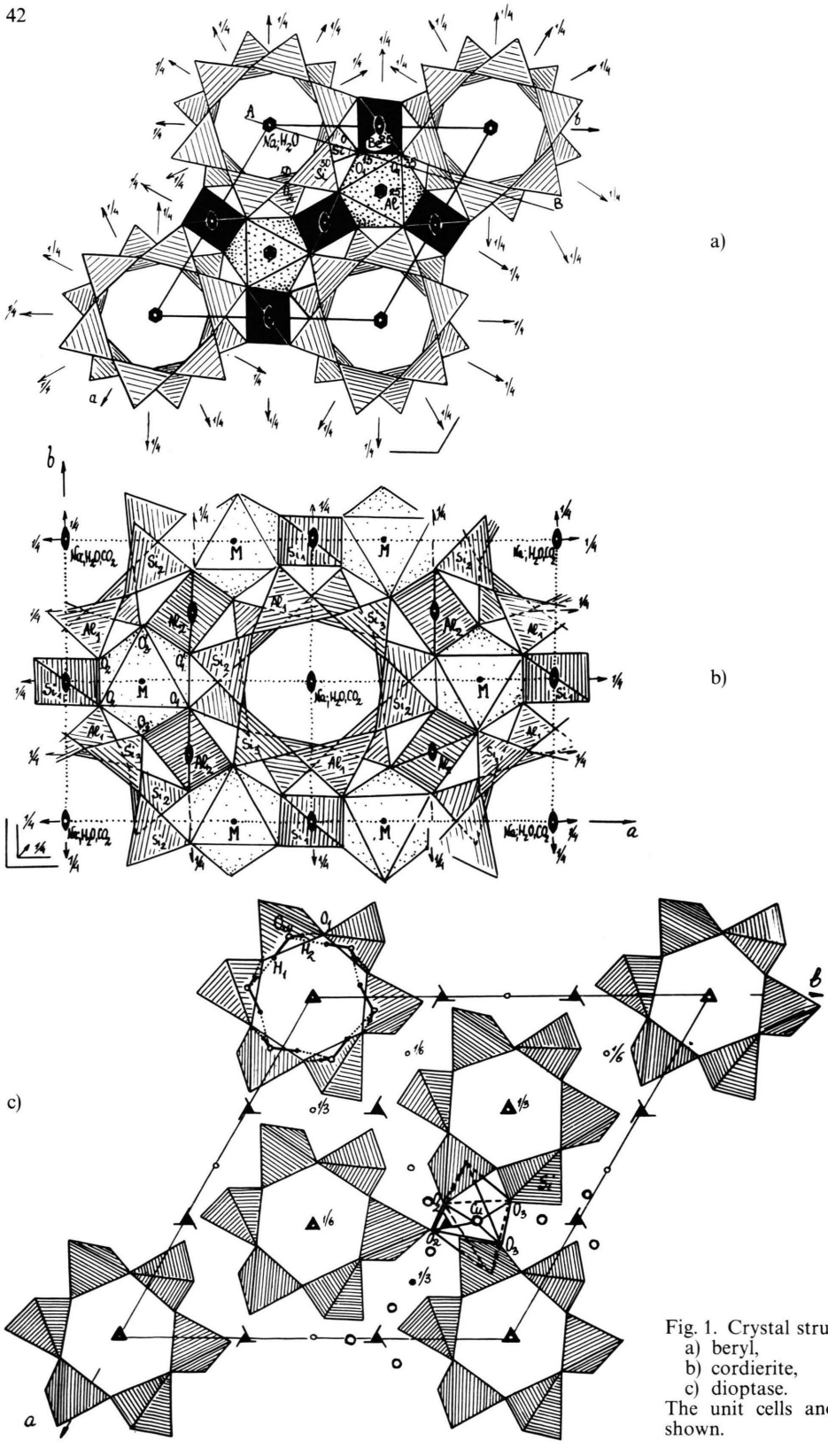

Fig. 1. Crystal structures in (001)-projection:
a) beryl,
b) cordierite,
c) dioptase.
The unit cells and symmetry elements are shown.

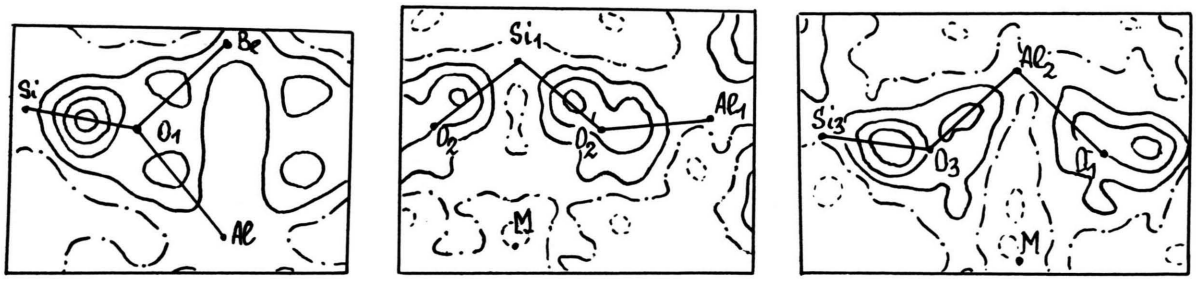

a) b) c)

Fig. 2. $\delta\varrho$-maps for identical structural fragments with 0.1 eÅ^{-3} contour interval: a) Si, Be-tetrahedra, Al-octahedron, $O_1-O'_1$ common edge (beryl), b) Al_1, Si_1, M, $O_2-O'_2$ (cordierite), c) Al_2, Si_3, M, O_3-O_1 (cordierite).

base for calculations of deformation electron density ($\delta\varrho$) maps (Figures 2–6). The $\sigma(\delta\varrho)$-maps were calculated in accordance with [8]. The values of errors on the atoms are for dioptase 0.4 eÅ^{-3} on Cu, 0.3 eÅ^{-3} on Si and 0.1 eÅ^{-3} on O, for cordierite 0.06 eÅ^{-3} on (Mg, Fe), 0.05 eÅ^{-3} on Si, 0.04 eÅ^{-3} on Al and 0.02 eÅ^{-3} on O, and for beryl 0.1 eÅ^{-3} on Si and Al, 0.02 eÅ^{-3} on Be and 0.05 eÅ^{-3} on O; in the region of chemical bonds the error is 0.1–0.2 eÅ^{-3}.

Let us consider the $\delta\varrho$-distribution of the three minerals: a) for the identical structural fragments, b) for different types of $[T_6O_{18}]$-rings, c) for H_2O molecules, and d) for octahedra with Al, (Mg, Fe) and Cu as central atoms. The latter deserves special interest owing to Jahn-Teller distortion.

The crystal structures of beryl and low-cordierite are very similar and have identical structural fragments. The reason for the lower symmetry (orthorhombic instead of hexagonal) of cordierite is considered to be the double substitution in the tetrahedra of the beryl crystal structure: two Si in the $[T_6O_{18}]$-ring by Al and three Be by two Al and one Si (Figures 1 a, b). The replacement of the central atoms in the tetrahedra and the octahedron in the structural fragment consisting of three polyhedra leads to remarkable differences in the $\delta\varrho$-maps for these two minerals (Figures 2 a–c). The $\delta\varrho$-maxima of 0.2 eÅ^{-3} on the Be–O bond in beryl (Fig. 2 a) are apparently displaced towards the oxygen atoms. Hence, Be–O σ-bonds have more polar character than the Si_1–O σ-bond in cordierite (Si_1 is situated in the Be-position), whereas the $\delta\varrho$-peak of 0.4 eÅ^{-3} (Fig. 2 b) lies in the middle of the bond. The same is true for the Al_2–O bond (Figure 2 c). In accordance with the change of the electronegativity of the elements we can also observe the $\delta\varrho$-redistribution around the oxygen: the small maximum of 0.1 eÅ^{-3} is on the (Mg, Fe)–O bond, the bigger maxima of 0.2–0.35 eÅ^{-3} are on Si, Al–O bonds (Figures 2 b, c). In contrast to cordierite, the $\delta\varrho$-peaks in beryl are almost equal (0.2 eÅ^{-3}) between Al–O in the octahedron and Be–O in the tetrahedron with increased concentration of $\delta\varrho$ (0.4 eÅ^{-3}) on Si–O bonds. It is possible to recognize on $\delta\varrho$-maps Si–O (0.35–0.4 eÅ^{-3}) and Al–O (0.20–0.25 eÅ^{-3}) bonds in cordierite, whereas in the $[Al_2Si_4O_{18}]$-ring the $\delta\varrho$-maxima on the bonds are "averaged".

Three $[T_6O_{18}]$-rings with different symmetry are presented on Figures 3 a–c. The puckered dioptase ring was collected from Si–O–Si′ fragments. The general rule for the $\delta\varrho$-distribution in $[T_6O_{18}]$-units is the electron density accumulation near the bridge oxygens. The values of $\delta\varrho$-peaks 0.3–0.4 eÅ^{-3} are nearly equal in highly symmetrical beryl-rings and correlate with bond lengths (Table 2). The $\delta\varrho$-map in cordierite has a more dispersed appearance, in agreement with the lower symmetry and the presence of both Si and Al atoms in the ring. The $\delta\varrho$-maxima on the bridge oxygens in dioptase are much higher (0.6–0.8 eÅ^{-3}; the shorter Si–O_1 bond corresponds to the largest maxima) than the ones in the first two minerals. On the other hand, comparison of the $\delta\varrho$-maxima near bridge and nonbridge oxygens inside $[TO_4]$-tetrahedra in beryl and cordierite shows the absence of any significant difference (Figures 4 a–c). In contrast to cordierite, in dioptase this difference is remarkable (0.2–0.3 eÅ^{-3}, Figure 4 e). This has apparently crystal chemical reasons. According to Godovikov [10], beryl and cordierite can be classified as framework structures formed by linkage of Si-, Al- and Be-tetrahedra. The $[Si_6O_{18}]$-units in the dioptase crystal structure are completely isolated from each other. The redistribution of $\delta\varrho$ inside the $[SiO_4]$-tetra-

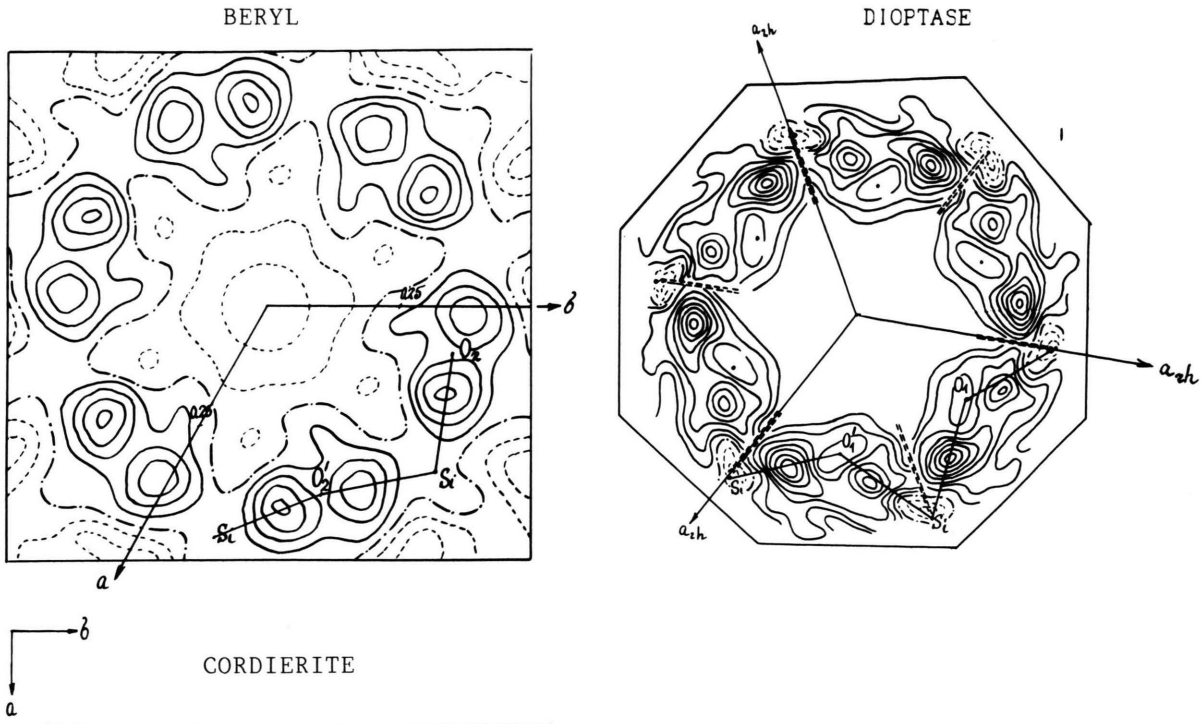

Fig. 3. $\delta\varrho$-maps through the $[T_6O_{18}]$-rings with 0.1 eÅ^{-3} contour interval: a) beryl, symmetry 6/m; b) cordierite, symmetry 2/m; c) dioptase, symmetry 3, line border double-dotted.

hedra in favour of the bridge oxygen is necessary in order to maintain the puckered pure ring-silicate unit for the rigidity of the structure, though with more effort.

The H_2O-molecules in beryl and cordierite have the same structural position in the channel (Figures 1 a, b). They are disordered, as it follows from $\delta\varrho$-maxima on O–H bonds and in accordance with the point symmetry of the O_w-position (622 in beryl and 222 in cordierite). Note that the planes of H_2O molecules are perpendicular to the *c*-axis in both structures.

The 6 H_2O-ring in dioptase is sandwiched between pairs of $[Si_6O_{18}]$-rings; together they form crown-shaped clusters with threefold symmetry (Figure 1 c). The experimental $\delta\varrho$-maps of H_2O molecules in dioptase (Figs. 5 a, b) are in good agreement with theoretical ones for the free molecule [11]. The difference in $\delta\varrho$-maxima on O–H bonds (0.6 eÅ^{-3}) and lone-pairs (0.4 eÅ^{-3}) can be explained if superposition effects are taken into account, which leads to an apparent decrease of the $\delta\varrho$ of H_2O lone-pairs in the crystal. The thermal motion is the other reason of this difference in $\delta\varrho$.

The $\delta\varrho$-maps of the $O_w-O_{w'}$ bond (Table 2) in the 6 H_2O-ring are in good agreement with theoretical ones [13], calculated for the same distance of about 2.6 Å.

The water-molecule rings have ice-like configuration, although the lone-pair positions are different in ice and dioptase: they are statistically disordered in the former and ordered outside the ring in the latter.

Table 2. The main interatomic distances (Å) in polyhedra and hydrogen bonds.

Beryl		Cordierite		Dioptase	
Be-tetrahedron		Si_1-tetrahedron		Si-tetrahedron	
$Be-O_1 \times 4$	1.657 (1)	$Si_1-O_2 \times 4$	1.630 (1)	$Si-O_1$	1.615 (2)
Si-tetrahedron		Si_2-tetrahedron		$O_{1'}$	1.651 (2)
$Si-O_1 \times 2$	1.623 (1)	$Si_2-O_1 \times 2$	1.638 (1)	O_2	1.596 (2)
O_2	1.595 (1)	O_5	1.587 (1)	O_3	1.528 (2)
$O_{2'}$	1.600 (1)	O_6	1.609 (1)		
				Cu-octahedron	
				$Cu-O_2$	1.937 (2)
Al-octahedron		Si_3-tetrahedron		$O_{2'}$	1.857 (1)
$Al-O_1 \times 6$	1.909 (1)	$Si_3-O_3 \times 2$	1.640 (1)	O_3	1.880 (1)
		O_4	1.574 (1)	$O_{3'}$	1.989 (2)
		O_6	1.616 (1)	O_w	2.464 (4)
				$O_{w'}$	2.633 (4)
		Al_1-tetrahedron			
		$Al_1-O_2 \times 2$	1.776 (1)		
		O_4	1.710 (1)	Hydrogen bonds	
		O_5	1.609 (1)	$O_w \ldots O_{w'}$	2.684 (6)
				O_w-H_1	0.970 (4)
		Al_2-tetrahedron		$H_1 \quad O_w$	1.773 (4)
		$Al_2-O_1 \times 2$	1.758 (1)	$O_w \quad O_1$	2.635 (4)
		$O_3 \times 2$	1.755 (1)	O_w-H_2	0.904 (5)
				$H_2 \quad O_1$	1.741 (2)
		M-octahedron		H_1-H_2	1.524 (1)
		$M-O_1 \times 2$	2.121 (1)	$\sphericalangle O_w-H_1-O_{w'}$	115.0 (2)°
		$O_2 \times 2$	2.126 (1)	$\sphericalangle O_w-H_2-O_1$	169.8 (2)°
		$O_3 \times 2$	2.133 (1)	$\sphericalangle H_1-O_w-H_2$	108.8 (4)°

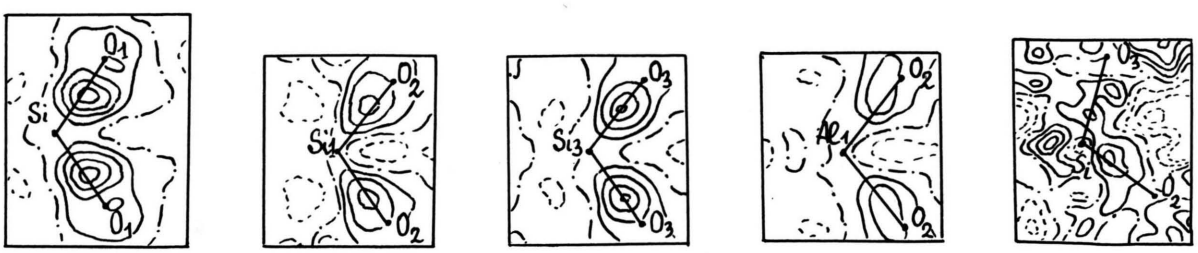

a) b) c) d) e)

Fig. 4. $\delta\varrho$-maps for $[TO_4]$-tetrahedra with nonbridging oxygens at 0.1 eÅ^{-3} contour interval: a) beryl, b–d) cordierite, e) dioptase.

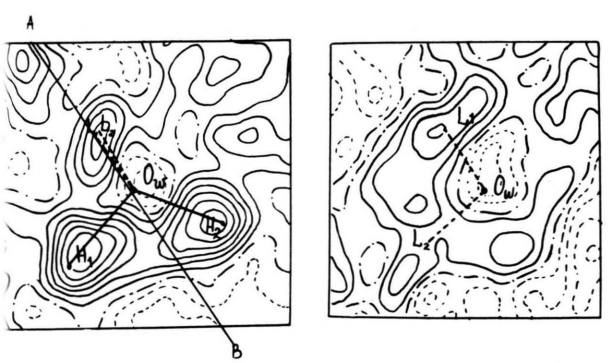

Fig. 5. $\delta\varrho$-maps of the H_2O molecule in dioptase with 0.1 eÅ^{-3} contour interval: a) $H_1-O_w-H_2$ plane, b) section perpendicular to the $H_1-O_w-H_2$ plane. A–B is the trace of this section. L_1, L_2 are ideal lone-pair positions.

The Cu-octahedron in dioptase shows Jahn-Teller distortion (Table 2) with four equatorial oxygen atoms and two apical water molecules. The 3d energy levels of Cu^{2+} in a field of tetragonal symmetry D_{4h} split into four sublevels: $e_g(d_{xz}, d_{yz})$, $b_{2g}(d_{xy})$, $b_{1g}(d_{x^2-y^2})$, $a_{1g}(d_{z^2})$. The $\delta\varrho$-maxima of 0.2–0.3 eÅ^{-3} (Figs. 6a, b) on Cu–O lines near oxygens can be considered as indication of a σ-bond. The smeared $\delta\varrho$-peak of 0.6 eÅ^{-3} (Fig. 6b) directed towards O_w is connected with the a_{1g}-level and partially with the e_g-level. Four $\delta\varrho$-minima directed towards the equatorial O ligands are connected with the b_{1g}-level, which is less occupied by electrons (Fig. 6a). Four $\delta\varrho$-maxima of 0.2–0.6 eÅ^{-3} in the same section are connected with the b_{2g}-

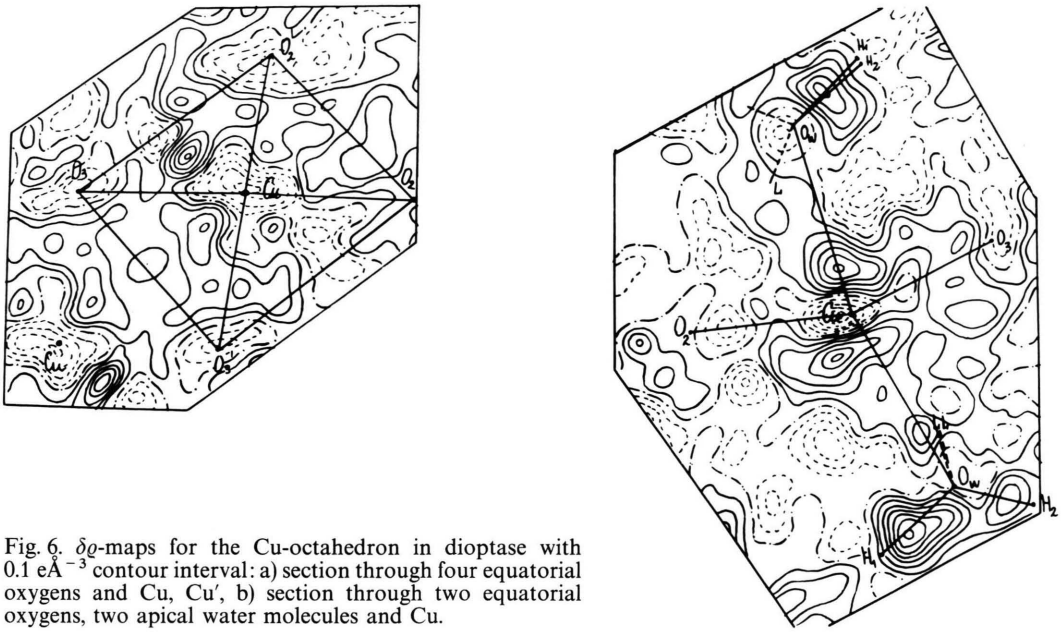

Fig. 6. $\delta\varrho$-maps for the Cu-octahedron in dioptase with 0.1 eÅ^{-3} contour interval: a) section through four equatorial oxygens and Cu, Cu′, b) section through two equatorial oxygens, two apical water molecules and Cu.

level. The difference in the values may be explained by the electrostatic interaction with ions from the second coordination sphere. The largest maximum of 0.6 eÅ^{-3} is observed near the O_3–$O_{2'}$ edge screened outside by two silicon atoms from the $[Si_6O_{18}]$-ring. The main features of the $\delta\varrho$-distribution in the Cu Jahn-Teller octahedron in dioptase are close to that in chalkantite $CuSO_4 \cdot 5\,H_2O$ [14].

Acknowledgements

The authors wish to express special thanks to Professor W. Weyrich, who organized and supported our participation at the Sagamore X Conference with the help of the Deutscher Akademischer Austauschdienst (DAAD). Thanks are also due to Professor V. S. Urusov for cooperation in this work.

[1] V. G. Tsirel'son and R. P. Ozerov, Electron density and bonding in crystals, Adam Hilger, Bristol 1992.
[2] V. G. Tsirel'son, O. A. Evdokimova, E. L. Belokoneva, and V. S. Urusov, Phys. Chem. Miner. **17,** 275 (1990).
[3] O. A. Evdokimova, E. L. Belokoneva, V. G. Tsirel'son, and V. S. Urusov, Geokhimia (Russ.) **1988,** 677.
[4] H. Strunz, Mineralogische Tabellen, Akademische Verlagsgesellschaft Geest & Portig K.-G., Leipzig 1977.
[5] Th. Armbruster, Amer. Mineral. **71,** 746 (1986).
[6] Th. Armbruster and H. B. Bürgi, Fortschr. Mineral. **60,** 37 (1982).
[7] N. V. Belov, B. A. Maksimov, Yu. Z. Nozik, and L. A. Muradyan, Doklady Akad. Nauk (Russ.) **239,** 842 (1978) and Sov. Phys. Doklady **23,** 215 (1978).
[8] N. N. Lobanov, V. G. Tsirel'son, and B. N. Shchedrin, Kristallografiya (Russ.) **35,** 589 (1990) and Sov. Phys. Crystallography **35,** 344 (1990).
[9] R. G. Gerr et al., Zh. Strukt. Khim. (Russ.) **32,** 171 (1991) and J. Struct. Chem. **32,** 146 (1991).
[10] A. A. Godovikov, Mineralogiya, Nedra, Moscow 1983.
[11] M. P. C. M. Krijn and D. Feil, Chem. Phys. **85,** 1 (1983).
[12] I. Olovsson, H. Ptasiewicz-Bak, and G. J. McIntyre, Z. Naturforsch. **48a,** 3 (1993).
[13] K. Hermansson, Acta Cryst. **B41,** 161 (1985).
[14] J. N. Vargese and E. N. Maslen, Acta Cryst. **B41,** 184 (1985).